ISSN 1674-1056
http://cpb.iphy.ac.cn
http://iopscience.iop.org/cpb
中国物理 B
Chinese Physics
中国物理
Chinese Physics B

Topological phases of a non-Hermitian coupled SSH ladder

J S Liu(刘建森), Y Z Han(韩炎桢), C S Liu(刘承师)
Citation: Chin. Phys. B . 2019, 28(10): 100304 . **doi:** 10.1088/1674-1056/ab3f94
Journal homepage: http://cpb.iphy.ac.cn; http://iopscience.iop.org/cpb

What follows is a list of articles you may be interested in

Phase diagram of interacting fermionic two-leg ladder with pair hopping

Wan-Li Liu(刘万里), Tian-Zhong Yuan(原天忠), Zhi Lin(林志), Wei Yan(闫伟)
Chin. Phys. B . 2019, 28(2): 020303 . **doi:** 10.1088/1674-1056/28/2/020303

Ultra-thin and light-weight spoof surface plasmon polariton coupler achieved by broadside coupled split ring resonators

Ya Fan(范亚), Jia-Fu Wang(王甲富), Hua Ma(马华), Yong-Feng Li(李勇峰), Ming-De Feng(冯明德), Shao-Bo Qu(屈绍波)
Chin. Phys. B . 2018, 27(10): 100304 . **doi:** 10.1088/1674-1056/27/10/100304

Observation of geometric phase in a dispersively coupled resonator-qutrit system

Libo Zhang(张礼博), Chao Song(宋超), H Wang(王浩华), Shi-Biao Zheng(郑仕标)
Chin. Phys. B . 2018, 27(7): 070303 . **doi:** 10.1088/1674-1056/27/7/070303

Tunable two-axis spin model and spin squeezing in two cavities

Lixian Yu(俞立先), Caifeng Li(李彩凤), Jingtao Fan(樊景涛), Gang Chen(陈刚), Tian-Cai Zhang(张天才), Suotang Jia(贾锁堂)
Chin. Phys. B . 2016, 25(5): 050301 . **doi:** 10.1088/1674-1056/25/5/050301

Topological phase transitions driven by next-nearest-neighbor hopping in noncentrosymmetric cold Fermi gases

Wang Rui, Zhang Cun-Xi, Ji Qing-Shan
Chin. Phys. B . 2015, 24(3): 030305 . **doi:** 10.1088/1674-1056/24/3/030305

Topological phases of a non-Hermitian coupled SSH ladder*

J S Liu(刘建森), Y Z Han(韩炎桢), and C S Liu(刘承师)†

Hebei Key Laboratory of Microstructural Material Physics, School of Science, Yanshan University, Qinhuangdao 066004, *China*

(Received 21 June 2019; revised manuscript received 8 August 2019; published online 25 September 2019)

We study topological phases of a non-Hermitian coupled Su–Schrieffer–Heeger (SSH) ladder. The model originates from the brick-wall lattices in the two-row limit. The Hamiltonian can be brought into block off-diagonal form and the winding number can be defined with the determine of the block off-diagonal matrix. We find the determine of the off-diagonal matrix has nothing to do with the interleg hopping of the ladder. So the topological phases of the model are the same as those of the chains. Further numerical simulations verify the analysis.

Keywords: topological phase, non-Hermitian, Su–Schrieffer–Heeger (SSH) ladder, winding number

PACS: 03.65.Vf, 05.70.Fh, 64.70.Tg **DOI:** 10.1088/1674-1056/ab3f94

1. Introduction

A number of recent works have started to explore the topological properties of non-Hermitian systems,[1–31] since non-Hermitian effects are found applicable in a wide range of systems including open boundaries[32–40] and systems with gain and/or loss.[25,41–57] Interestingly, non-Hermitian Hamiltonian exhibits the intriguing features and many other interesting phenomena with no counterpart in Hermitian cases, e.g., the existence of exceptional points where the Hamiltonian becomes nondiagonalizable.[25,58] A key issue of non-Hermitian systems is to find the topological invariants which are responsible for the bulk–boundary correspondence. Previous non-Hermitian topological invariants, including the Chern number, generalized Berry phase, and winding number, are formulated in terms of the Bloch Hamiltonian by employing the biorthonormal eigenvectors.[1–7,9,48] However, numerical results in a one-dimensional (1D) model show that open-boundary spectra look quite different from periodic-boundary ones, which seems to indicate that the bulk topological invariants fail to be responsible for the topological edge states.[2,6]

To establish the non-Hermitian bulk–boundary correspondence, one possible way is to find a Hermitian counterpart of the corresponding non-Hermitian Hamiltonian. The Hermitian Hamiltonian can be constructed with a pseudo-Hermiticity operator. A Hermitian counterpart can have an identical fully real spectrum in the symmetry-unbroken region.[5,59–61] The other case is taking the non-Hermitian skin effect into account, where the bulk states are localized at boundaries and deviate from the extended Bloch waves. The non-Hermitian skin effect is from asymmetric tunneling amplitudes which create effectively an imaginary gauge field. Nonzero imaginary magnetic flux breaks the conventional bulk–boundary correspondence and leads to a topological phase transition.[62,63] A non-Bloch topological invariant is introduced and gives the number of topological edge modes of the non-Hermitian Hamiltonian.[63–67]

The coupled Su–Schrieffer–Heeger (SSH) systems, as the crossover from one-dimensional (1D) to two-dimensional (2D) system, host a rich phase diagram which is different from that of both 1D and 2D systems.[68–70] Then for the non-Hermitian version of the SSH ladder, what is the bulk–boundary correspondence and what is the topological invariant that determines the zero modes? In a study of the model, the winding number was defined in the generalized Brillouin zone (GBZ) and faithfully predicted the topological zero-energy edge modes.[71] We study a special non-Hermitian version of the coupled SSH model which originates from the two-row limit of the brick-wall lattices. Benefiting from the existence of the complex wave vector in GBZ, we can define the winding number in GBZ without solving the model directly. It is found that the winding number has nothing to do with the interleg hopping. The two chains are decoupled completely. We can obtain the topological phase transition point from the studies in Ref. [64]. The numerical analysis is used to verify our study.

The remainder of this paper is organized as follows. In Section 2, we present the coupled-SSH chains and explain the origination of the model. Section 3 gives the theoretical and numerical analysis to prove that the interleg hopping does not modify the topological feature of the model. The phase diagram of the model is the same as that of the chain. Finally, we present a summary and discussion in Section 4.

2. Models

The system is coupled SSH chains with the two-leg ladder structure. The geometry of the system is sketched in Fig. 1(a).

*Project supported by Hebei Provincial Natural Science Foundation of China (Grant Nos. A2012203174 and A2015203387) and the National Natural Science Foundation of China (Grant Nos. 10974169 and 11304270).

†Corresponding author. E-mail: csliu@ysu.edu.cn

© 2019 Chinese Physical Society and IOP Publishing Ltd

Each ladder is a bipartite lattice system, consisting of two sublattices a and b (or c and d). The hopping amplitudes in each leg are staggered and the rung indicates the interleg hopping. The model originates from the two-row limit of the brick-wall lattice [Fig. 1(b)] which is an alternative representation of the honeycomb lattice [Fig. 1(c)].

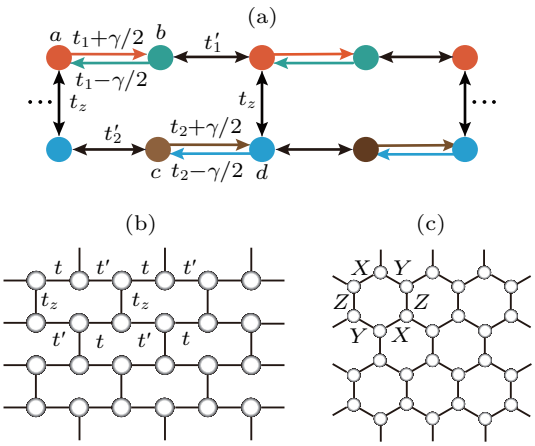


Fig. 1. (a) Coupled SSH chains which are the two-row limit of the brick-wall lattice. (b) The brick-wall lattice is equivalent to (c) the honeycomb lattice.

The model is described by the Hamiltonian

$$\begin{aligned} H &= \psi^{\dagger}\mathcal{H}\psi \\ &= \sum_j \left[t_{1,\mathrm{L}}a_j^{\dagger}b_j + t_{1,\mathrm{R}}b_j^{\dagger}a_j + t_1'a_{j+1}^{\dagger}b_j + t_1'b_j^{\dagger}a_{j+1}\right] \\ &\quad + \sum_j \left[t_{2,\mathrm{L}}c_j^{\dagger}d_j + t_{2,\mathrm{R}}d_{j+1}^{\dagger}c_j + t_2'c_{j+1}^{\dagger}d_j + t_2'd_j^{\dagger}c_{j+1}\right] \\ &\quad + \sum_j t_z\left(a_j^{\dagger}d_j + d_j^{\dagger}a_j\right), \end{aligned} \tag{1}$$

where $a_j^{\dagger}$ (a_j) and $b_j^{\dagger}$ (b_j) are the electron creation (annihilation) operators on the sublattices 1 of the j-th unit cell, respectively. $c_j^{\dagger}$ (c_j) and $d_j^{\dagger}$ (d_j) are the electron creation (annihilation) operators on the sublattices 2 of the j-th unit cell, respectively. The creation operator is $\psi^{\dagger} = \left(a_1^{\dagger}, b_1^{\dagger}, \ldots, a_N^{\dagger}, b_N^{\dagger}, c_1^{\dagger}, d_2^{\dagger}, \ldots, c_N^{\dagger}, d_N^{\dagger}\right)$.

The non-Hermiticity of the Hamiltonian $\mathcal{H}$ in Eq. (1) is due to the introduction of $\gamma/2$ which changes the hopping term in the unit cell with different hopping strengths $t_{i,+} = t_i + \gamma_i/2$ in the right direction and $t_{i,-} = t_i - \gamma_i/2$ in the left direction ($i = 1, 2$). By adopting periodic boundary conditions and Fourier transform $\psi_j = 1/N\sum_k \mathrm{e}^{\mathrm{i}kj}\psi_k$ ($\psi = a, b, c, d$), the Hamiltonian H can be easily written as $H = \sum_k \psi_k^{\dagger}h_k\psi_k$, and

$$h_k = \begin{pmatrix} 0 & \zeta_{1,k,+} & 0 & t_z \\ \zeta_{1,k,-}^{*} & 0 & 0 & 0 \\ 0 & 0 & 0 & \zeta_{2,k,+} \\ t_z & 0 & \zeta_{2,k,-}^{*} & 0 \end{pmatrix}, \tag{2}$$

with $\zeta_{i,k,\pm} = t_i'\mathrm{e}^{-\mathrm{i}k} + t_{i,\pm}$. The Hamiltonian h_k has a chiral symmetry $\Sigma_z^{\dagger}h_k\Sigma_z = -h_k$ with $\Sigma_z = \sigma_z\sigma_z$. The chiral symmetry ensures the eigenvalues in $[E, -E]$ pairs.

3. Results

The non-Hermitian skin effect determines drastically the topology of the non-Hermitian systems. The non-Bloch bulk–boundary correspondence and generalized Brillouin zone were suggested in the discussion in Refs. [64], [66], [71], and [72]. In the generalized Brillouin zone, the wave number k becomes complex. The real part of the wave vector is from the the periodicity of the system according to the Bloch theorem. The non-Hermitian skin effect attributes to the imaginary part of the complex-valued wave vector. The non-Hermitian topological invariant can be constructed by replacing the Bloch phase factor $\mathrm{e}^{\mathrm{i}k}$ by β ($\mathrm{e}^{\mathrm{i}k} \to \beta, \mathrm{e}^{-\mathrm{i}k} \to 1/\beta$) and the value of $\beta \equiv \mathrm{e}^{\mathrm{i}k}$ is confined in a loop on the complex plane. The $-\mathrm{i}$ time of natural logarithm values $k \to -\mathrm{i}\ln\beta$ form a generalized Brillouin zone (GBZ), where $|\beta|$ is generally not a unit circle in the complex plane. The GBZ and E can be obtained by solving the equation $|\beta_i(E)| = |\beta_j(E)|$, where i, j are the middle two indexes when ordering $|\beta_i(E)|$ as $|\beta_1(E)| \leq |\beta_2(E)| \leq \cdots \leq |\beta_N(E)|$.

The existence of β gives an opportunity to find the non-Bloch topological invariants of the model according to the results given in Ref. [64] without solving the model directly. With the unitary

$$U = \begin{pmatrix} 0 & 0 & 0 & 1 \\ 0 & 1 & 0 & 0 \\ 0 & 0 & 1 & 0 \\ 1 & 0 & 0 & 0 \end{pmatrix},$$

the Hamiltonian h_β in Eq. (2) is brought into block off-diagonal form by the unitary transformation

$$\bar{H} = Uh_\beta U^{-1} = \begin{pmatrix} 0 & V_1 \\ V_2 & 0 \end{pmatrix},$$

where

$$V_1 = \begin{pmatrix} \zeta_{2,\beta,-}^{*} & t_z \\ 0 & \zeta_{1,\beta,-,}^{*} \end{pmatrix}, \quad V_2 = \begin{pmatrix} \zeta_{2,\beta,+} & 0 \\ t_z & \zeta_{1,\beta,+} \end{pmatrix}. \tag{3}$$

The determinants of V_1 and V_2 are $q_1 = \mathrm{Det}V_1 = \zeta_{1,\beta,-}^{*}\zeta_{2,\beta,-}^{*}$ and $q_2 = \mathrm{Det}V_2 = \zeta_{1,\beta,+}\zeta_{2,\beta,+}$ which have nothing to do with t_z. With the determinants q_1 and q_2 as the winding vectors, the winding number is defined by

$$\mathcal{W} = \frac{\mathrm{i}}{2\pi}\int_{c_\beta} q_1^{-1}\,\mathrm{d}q_1 = \frac{\mathrm{i}}{2\pi}\int_{c_\beta} q_2^{-1}\,\mathrm{d}q_2, \tag{4}$$

which is defined on the GBZ. The winding numbers of the winding vectors q_1 and q_2 on the GBZ c_β can be used as topological invariants to distinguish the different topological nontrivial states.

When $\gamma_1 = \gamma_2 = 0$, the non-Hermitian skin effect disappears and the Hamiltonian in Eq. (2) becomes Hermitian. In such case, the wave vector is real quantum according the

Bloch theorem. The winding number defined by the block off-diagonal Hamiltonian in Eq. (3) is still effective to distinguish the topological nontrivial phase and has nothing to do with t_z. The conventional bulk–boundary correspondence governs the system.

From Eq. (4), the winding number has nothing to do with t_z. It gives us a strong evidence that the two ladders are decoupled completely when discussing the topological behaviors. The augment is first reported for the Hermitian SSH ladder in Ref. [73]. Here, we obtain the argument in the non-Hermitian case which benefits from the the existence of the generalized Brillouin zone. To verify the above analysis, we diagonalize $\mathcal{H}$ in Eq. (1) under the open boundary condition. The parameters are $t_1 = 1.3$, $t_2 = 0.4$, $t_z = 1.2$, $\gamma_1 = 4/3$, and $\gamma_2 = 2/3$. The intercell hoppings are taken to be $t_1' = t_2' = t'$. As shown in Fig. 2(a), the energies as a function as t' are completely real-valued. The zero modes exist for $|t'| \geq 1.1160$ and $|t'| \leq 0.4989$. We have changed t_z and re-calculated the energies as a function of t'. It is found that the energies change obviously and the zero modes remain unchanged, however. To understand the four phase transition points at $|t'| = 1.1160$ and $|t'| = 0.4989$, we diagonalize the two ladders which are non-Hermitian SSH models, respectively. The absolute values of energies as function as t' are shown in Figs. 2(b) and 2(c). Shown by four vertical lines, the four phase transition points are the same as those of individual non-Hermitian SSH I and II. The topological phase transition points have been analytically solved in Ref. [64] for the non-Hermitian SSH chain. The transition points are $\sqrt{t_i^2 - \gamma_i^2/4} = t_i'$ for the two ladders respectively. With the parameters used in Fig. 2, the transition points are $t' = \pm 0.4989$ and ± 1.1160.

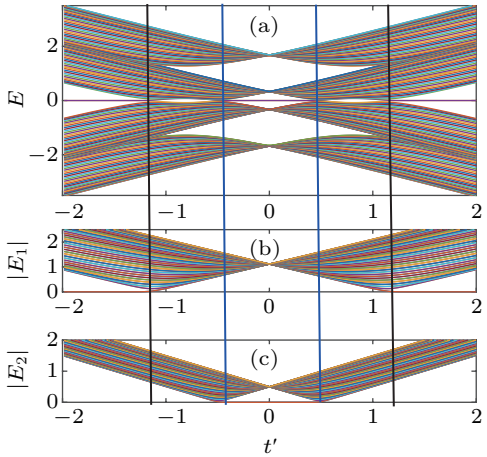


Fig. 2. Energy spectra of an open chain with length $L = 80$ (unit cell) as a function of t' by numerical diagonalization of the Hamiltonian: (a) $\mathcal{H}$ in Eq. (1), (b) of the non-Hermitian SSH model for ladder I, (c) of the non-Hermitian SSH model for ladder II. Here $t_1 = 1.3$, $t_2 = 0.6$, $t_z = 1.2$, $\gamma_1 = 4/3$, and $\gamma_2 = 2/3$. The other parameters are set to be $t_1' = t_2' = t'$.

To further understand the model and the non-Hermitian skin effect, we carry out the following similarity transformation $\bar{\mathcal{H}} = S^{-1}\mathcal{H}S$ and $|\bar{\Psi}\rangle = S^{-1}|\Psi\rangle$ with $\bar{\Psi}^\dagger = \left(\bar{a}_1^\dagger, \bar{b}_1^\dagger, \ldots, \bar{a}_N^\dagger, \bar{b}_N^\dagger, \bar{c}_1^\dagger, \bar{d}_2^\dagger, \ldots, \bar{c}_N^\dagger, \bar{d}_N^\dagger\right)$ as done in Ref. [64]. For simplicity, the parameters are set to be $t_1 = t_2 = t$ and $\gamma_1 = \gamma_2$. S can be a diagonal matrix whose diagonal elements are $\{1, r, r, r^2, r^2, \ldots, r^{L-1}, r^{L-1}, r^L, 1, 1, r, r, r^2, r^2, \ldots, r^{L-1}, r^{L-1}\}$. After the transformation, the model is described by the Hamiltonian

$$\begin{aligned}\bar{H} &= \bar{\psi}^\dagger \bar{\mathcal{H}} \bar{\psi} \\ &= \sum_j \left[\bar{t}\bar{a}_j^\dagger b_j + \bar{t}\bar{b}_j^\dagger \bar{a}_j + t'\bar{a}_{j+1}^\dagger \bar{b}_j + t'\bar{a}_{j+1}^\dagger \bar{b}_j\right] \\ &\quad + \sum_j \left[\bar{t}\bar{c}_j^\dagger \bar{d}_j + \bar{t}\bar{d}_{j+1}^\dagger \bar{c}_j + t'\bar{c}_{j+1}^\dagger \bar{d}_j + t'\bar{d}_{j+1}^\dagger \bar{c}_j\right] \\ &\quad + \sum_j t_z\left(\bar{a}_j^\dagger \bar{d}_j + \bar{d}_j^\dagger \bar{a}_j\right). \end{aligned} \tag{5}$$

If we take $r = \sqrt{|(t-\gamma/2)/(t+\gamma/2)|}$, $\bar{H}$ is the coupled SSH model, with the intracell hopping $\bar{t} = \sqrt{(t-\gamma/2)(t+\gamma/2)}$. The intercell hopping t' and inter-chain hopping t_z remain unchanged.

The open-boundary spectra of Hamiltonian $\mathcal{H}$ in Eq. (2) and $\bar{\mathcal{H}}$ in Eq. (5) are given in Figs. 3(a) and 3(b), respectively. The open chain length is $L = 80$. The other parameters are taken to be $t_2 = 1$, $\gamma = 4/3$, and $t_z = 0.3$. It is interesting to see that the zero modes exist in $-3 < t < 3$. This is due to the decoupled two chains and the transition points at $\bar{t} = t'$, i.e., $t = \sqrt{t'^2 + (\gamma/2)^2}$. When $t > \sqrt{t'^2 + (\gamma/2)^2}$, one chain has the zero-energy modes. When $t < \sqrt{t'^2 + (\gamma/2)^2}$, the other chain has the zero-energy modes however.

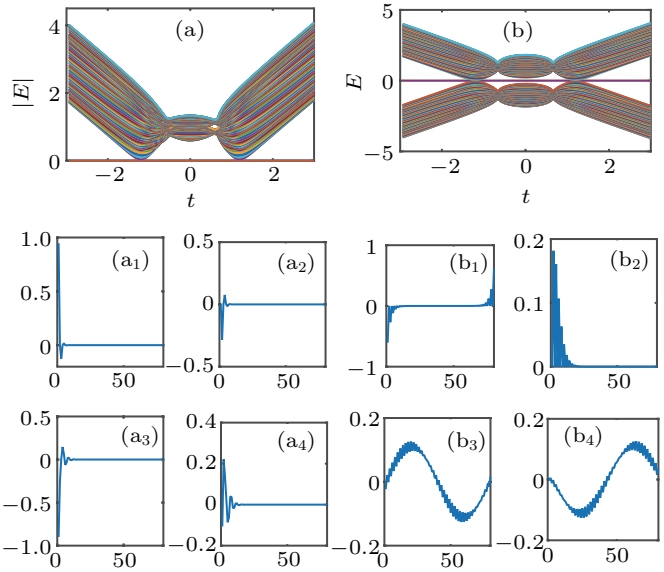


Fig. 3. (a) (b) The open-boundary spectra of Hamiltonian $\mathcal{H}$ in Eq. (5) and $\bar{\mathcal{H}}$ in Eq. (5). The parameters are taken to be $t_2 = 1$, $\gamma = 4/3$, and $t_z = 0.3$. Panels (a_1)–(b_4) show the eigenfunctions. The x-axis is the coordinate of the chain. Panels (a_1)–(a_4) are the non-Hermitian cases. Panels (b_1)–(b_4) are the Hermitian cases. Panels (a_1), (a_2), (b_1), (b_2) show the zero-energy modes of the two chains. Panels (a_3), (a_4), (b_3), (b_4) show the non-zero-energy modes of the two chains.

The wave functions are shown in Fig. 3 for $t = 0.8$. For the non-Hermitian case, figures 3(a_1) and 3(a_2) show the zero-energy modes, and figures 3(a_3) and 3(a_4) show the non-zero-energy modes. Due to the non-Hermitian skin effect, the eigenstates of one open chain [Figs. 3(a_1) and 3(a_3)] and the other chain [Figs. 3(a_2) and 3(a_4)] are found to be localized near the left boundary, which is in contrast to the Hermitian cases in Figs. 3(b_1)–3(b_4). Figures 3(b_1) and 3(b_2) show the zero-energy modes of the the Hermitian cases. The zero-energy mode in Fig. 3(b_1) of chain I is an asymmetry wave function duo to the symmetry of chain I. The zero-energy mode in Fig. 3(b_2) of chain II is a localized wave function since the chain II does not possess the symmetry. The non-zero-energy modes in Figs. 3(b_3) and 3(b_4) are all the extended Bloch waves in the two chains.

4. Summary

We have studied topological phases of a special non-Hermitian coupled SSH ladder where the interlegs of the special ladder are cancelled alternately. The model is different from the general ladder and originates from the brick-wall lattices in the two-row limit. With a unity transition, the Hamiltonian in GBZ is brought into block off-diagonal form. According to the calculations of the winding number defined by the determine of the block off-diagonal matrix, we find that the interleg hopping has nothing to do with the topological number of the ladder. So the special coupled SSH chain is decoupled when discussing the topological behavior. The topological properties of the model are determined by the single non-Hermitian SSH chain. This method may be useful to investigate other multi-leg ladder models.

References

[1] Esaki K, Sato M, Kazuki H and Kohmoto M 2011 *Phys. Rev. B* **84** 205128
[2] Lee T E 2016 *Phys. Rev. Lett.* **116** 133903
[3] Leykam D, Bliokh K Y, Huang C, Chong Y D and Nori F 2017 *Phys. Rev. Lett.* **118** 040401
[4] Lieu S 2018 *Phys. Rev. B* **97** 045106
[5] Li C, Zhang X Z, Zhang G and Song Z 2018 *Phys. Rev. B* **97** 115436
[6] Yin C H and Jiang H, Li L H, Lü R and Chen S 2018 *Phys. Rev. A* **97** 052115
[7] Shen H T, Zhen B and Fu L 2018 *Phys. Rev. Lett.* **120** 146402
[8] Liang S D and Huang G Y 2013 *Phys. Rev. A* **27** 012118
[9] Rudner M S and Levitov L S 2009 *Phys. Rev. Lett.* **102** 065703
[10] Kawabata K, Ashida Y, Katsura H and Ueda M 2018 *Phys. Rev. B* **98** 085116
[11] Gong J B and Wang Q H 2010 *Phys. Rev. A* **82** 012103
[12] Gong Z P, Higashikawa S and Ueda M 2017 *Phys. Rev. Lett.* **118** 200401
[13] Hu Y C and Hughes T L 2011 *Phys. Rev. B* **84** 153101
[14] Gonzalez J and Molina R A 2017 *Phys. Rev. B* **96** 045437
[15] Cerjan A, Xiao M, Yuan L and Fan S H 2018 *Phys. Rev. B* **97** 075128
[16] Zyuzin A A and Zyuzin A Y 2018 *Phys. Rev. B* **97** 041203
[17] Rivolta N X A, Benisty H and Maes, B 201 *Phys. Rev. A* **96** 023864
[18] Wang X H, Liu T T, Xiong Y and Tong, P Q 2015 *Phys. Rev. A* **92** 012116
[19] Klett M, Cartarius H, Dast D, Main J and Wunner G 2017 *Phys. Rev. A* **95** 053626
[20] Ni X, Smirnova D, Poddubny A, Leykam Daniel, Chong Y and Khanikaev A B 2018 *Phys. Rev. B* **98** 165129
[21] Zhou L W, Wang Q H, Wang H L and Gong J B 2018 *Phys. Rev. A* **98** 022129
[22] Yuce C 2015 *Phys. Lett. A* **379** 1213
[23] Ke S, Wang B, Long H, Wang K and Lu P 2017 *Opt. Express* **25** 011132
[24] Gong Z P, Ashida Y, Kawabata K, Takasan K, Higashikawa S and Ueda M 2018 *Phys. Rev. X* **8** 031079
[25] Hu W C, Wang H L, Shum P P and Chong Y D 2017 *Phys. Rev. B* **23** 094206
[26] Parto M, Wittek S, Hodaei H, Harari G, Bandres M, Ren J, Rechtsman M C, Segev M, Christodoulides D N and Khajavikhan M 2018 *Phys. Rev. Lett.* **120** 113901
[27] Zhan X, Xiao L, Bian Z H, Wang K K, Qiu X Z, Sanders B C, Yi W and Xue P 2017 *Phys. Rev. Lett* **119** 130501
[28] Zeuner J M, Rechtsman M C, Plotnik Y, Lumer Y, Nolte S, Rudner M S, Segev M and Szameit A 2015 *Phys. Rev. Lett.* **115** 040402
[29] Xiao L, Zhan X, Bian Z H, Wang K K, Zhang X, Wang X P, Li J, Mochizuki K, Kim D and Kawakami N 2017 *Nat. Phys.* **13** 1117
[30] Weimann S, Kremer, M. Plotnik, Y, Lumer, Y, Nolte S, Makris K G, Segev M, Rechtsman M C and Szameit A 2017 *Nat. Mater.* **16** 433
[31] Hengyun Z, Chao P, Yoseob Y, Chia W H, Keith A N, Liang F, John D J, Marin S and Bo Z 2018 *Science* **359** 1009
[32] Choi Y W, Kang S S, Lim S, Kim W, Kim J, Lee J and An K 2010 *Phys. Rev. Lett.* **104** 153601
[33] Cao H and Wiersig Jan 2015 *Rev. Mod. Phys.* **87** 61
[34] Malzard S, Poli C and Schomerus H 2015 *Phys. Rev. Lett.* **115** 200402
[35] Carmichael H J 1993 *Phys. Rev. Lett* **70** 2273
[36] Lee T E and Chan C K 2014 *Phys. Rev. X* **23** 094206
[37] Lee T E, Reiter F and Moiseyev N 2014 *Phys. Rev. Lett* **113** 250401
[38] Diehl S, Rico E, Baranov M A and Zoller P 2011 *Nat. Phys.* **7** 971
[39] Choi Y, Kang S, Lim S, Kim W, Kim J R, Lee J H and An K 2010 *Phys. Rev. Lett.* **104** 153601
[40] Han Y Z and Liu C S 2019 *Physica E* **108** 116
[41] Deng H, Haug H and Yamamoto Y 2010 *Rev. Mod.Phys.* **82** 1489
[42] Dattoli G, Hermsen T, Mezi L, Renieri A and Torre A 1988 *Phys. Rev. A* **37** 4334
[43] Makris K G, El-Ganainy R, Christodoulides D N and Musslimani Z H 2008 *Phys. Rev. Lett.* **100** 103904
[44] Longhi S 2009 *Phys. Rev. Lett.* **103** 123601
[45] Klaiman S, Gunther U and Moiseyev N 2008 *Phys. Rev. Lett.* **101** 084002
[46] Bittner S, Dietz B, Gunther U, Harney H L, Miski-Oglu M, Richter A and Schafer F 2012 *Phys. Rev. Lett.* **108** 024101
[47] Liertzer M, Ge Li, Cerjan A, Stone A D, Tureci H E and Rotter S 2012 *Phys. Rev. Lett* **108** 173901
[48] Menke H and Hirschmann M M 2017 *Phys. Rev. B* **95** 174506
[49] Yuce C 2016 *Phys. Rev. A* **93** 062130
[50] Klett M, Cartarius H, Dast D, Main J and Wunner G 2018 *Eur. Phys. J. D* **72** 214
[51] Regensburger A, Bersch C, Miri M A, Onishchukov G, Christodoulides D N and Peschel U 2012 *Nature* **488** 167171
[52] Rüter C E, Makris K G, Elganainy R, Christodoulides D N, Segev M and Kip D 2010 *Nat. Phys.* **6** 192
[53] Feng L, Wong Z J, Ma R M, Wang Y and Zhang X 2014 *Science* **346** 972
[54] Gao T, Estrecho E, Bliokh K Y, Liew T C H, Fraser M D, Brodbeck S, Kamp M, Schneider C, Hfling S and Yamamoto Y 2015 *Nature* **526** 554
[55] Ozawa T, Price H M, Amo A, Goldman N, Hafezi M, Lu L, Rechtsman M, Schuster D, Simon J and Zilberberg O 2018 *Rev. Mod. Phys.* **91** 015006
[56] Ling L, John D J and Marin S 2014 *Nat. Photon.* **8** 821

[57] Elganainy R, Makris K G, Khajavikhan M, Musslimani Z H, Rotter S and Christodoulides D N 2018 *Nat. Phys.* **14** 11
[58] Ingrid R 2009 *J. Phys. A-Math. Theor.* **42** 153001
[59] Bender C M and Boettcher S 1998 *Phys. Rev. Lett.* **80** 5243
[60] Mostafazadeh A 2002 *J. Math. Phys.* **43** 205
[61] Zhu B G, Lu R and Chen S 2014 *Phys. Rev. A* **89** 062102
[62] Wu H C and Jin L and Song Z 2019 arXiv 1905 11576
[63] Jin L and Song Z 2019 *Phys. Rev. B* **99** 081103
[64] Yao S Y and Wang Z 2018 *Phys. Rev. Lett.* **121** 086803
[65] Kawabata K, Shiozaki K and Ueda M 2018 *Phys. Rev. B* **98** 165148
[66] Yao S Y, Song F and Wang Z 2018 *Phys. Rev. Lett.* **121** 136802
[67] Deng T S and Yi W 2019 *Phys. Rev. B* **100** 035102
[68] Clay R T and Mazumdar S 2005 *Phys. Rev. Lett.* **94** 207206
[69] Shimizu Y, Aoyama S, Jinno T, Itoh M and Ueda Y 2015 *Phys. Rev. Lett.* **114** 166403
[70] Cheon S, Kim T, Lee S and Yeom H W 2015 *Science* **350** 182
[71] Song F, Yao S Y and Wang Z 2019 arXiv 1905 02211
[72] Kazuki Y and Shuichi M 2019 *Phys. Rev. Lett.* **123** 066404
[73] Li C, Lin S, Zhang G and Song Z 2019 *Phys. Rev. B* **96** 125418